



HAL
open science

Long-term thermo-mechanical behavior of energy pile in dry sand

van Tri Nguyen, Anh Minh A.M. Tang, Jean-Michel Pereira

► **To cite this version:**

van Tri Nguyen, Anh Minh A.M. Tang, Jean-Michel Pereira. Long-term thermo-mechanical behavior of energy pile in dry sand. *Acta Geotechnica*, 2017, 10.1007/s11440-017-0539-z . hal-01515976

HAL Id: hal-01515976

<https://enpc.hal.science/hal-01515976>

Submitted on 28 Apr 2017

HAL is a multi-disciplinary open access archive for the deposit and dissemination of scientific research documents, whether they are published or not. The documents may come from teaching and research institutions in France or abroad, or from public or private research centers.

L'archive ouverte pluridisciplinaire **HAL**, est destinée au dépôt et à la diffusion de documents scientifiques de niveau recherche, publiés ou non, émanant des établissements d'enseignement et de recherche français ou étrangers, des laboratoires publics ou privés.

[Click here to view linked References](#)

1 **Long-term thermo-mechanical behavior of energy pile in dry sand**

2 Van Tri NGUYEN^{(1),(2)}, Anh Minh TANG⁽¹⁾, Jean Michel PEREIRA⁽¹⁾

3 (1) *École des Ponts ParisTech, Laboratoire Navier, France*

4 (2) *Hanoi University of Mining and Geology, Vietnam*

5

6

7

8

9 Corresponding author:

10 Dr. Anh Minh TANG

11

12 Ecole des Ponts ParisTech

13 6-8 avenue Balaise Pascal, Cité Descartes, Champs-sur-Marne

14 77455 Marne-la-Vallée

15 France

16 Email : anhminh.tang@enpc.fr

17 Phone : +33 1 64 15 35 63

18 Fax : +33 1 64 15 35 62

19 **Abstract:** A small-scale pile has been developed in the laboratory to investigate the thermo-
20 mechanical behavior of energy piles subjected to a significant number of thermal cycles. The
21 model pile (20 mm external diameter), installed in dry sand, was initially loaded at its head to 0,
22 20, 40 and 60% of its ultimate bearing capacity (500 N). At the end of each loading step, 30
23 heating/cooling cycles were applied to the pile. The long-term behavior of the pile was observed
24 in terms of pile head settlement, axial force profile, soil and pile temperature, and stress in soil.
25 The results evidence the irreversible settlement of the pile head induced by thermal cycles under
26 constant load head. In addition, the incremental irreversible settlement, that accumulates after
27 each thermal cycle, decreases when the number of cycles increases. The evolution of irreversible
28 pile head settlement versus number of cycles can be reasonably predicted by an asymptotic
29 equation.

30

31 **Keywords:** energy pile, physical model, long-term behavior, heating/cooling cycles, thermo-
32 mechanical load

33 **1. Introduction**

34 Energy piles, or heat exchanger piles, have a dual function: (i) providing support for overhead
35 structures as a conventional pile foundation; (ii) and exchanging heat with the ground for the
36 purpose of heating and/or cooling the building. Energy piles have been used in some European
37 countries during the last two decades. This technique has gained encouraging credit as an option
38 to the use of renewable energy in modern cities and contributed to the reduction of CO₂
39 emissions [1–3]. However, the implementation of this technique is not homogeneous across
40 countries due to the lack of design standards.

41
42 Many studies have been carried out to investigate the thermo-mechanical behavior of energy
43 piles [2, 4–30]. Some involved in situ full-scale experiments [2, 4, 11, 27, 31, 32] or laboratory
44 small-scale experiments [7, 14, 18, 21, 22, 24, 25]. The results evidence the effect of pile
45 temperature on the pile/soil interaction. Indeed, the temperature of energy piles can vary in the
46 range of 5°C to 40°C and can thus induce stress changes along the pile and movement of the pile
47 head. These phenomena are the consequences of the pile thermal dilation/contraction and the
48 effect of temperature on the behavior of the pile/soil interface. The above mechanisms were
49 considered in various numerical studies to predict the behavior of energy piles under thermo-
50 mechanical loadings [2, 9, 10, 12, 17, 29, 30, 33–38].

51
52 In spite of various studies on the thermo-mechanical behavior of energy piles, few works have
53 investigated their long-term behavior. Actually, to deal with this aspect, some studies
54 investigated the mechanical behavior of energy piles under numerous thermal cycles, which
55 represent the seasonal variations of the pile temperature. Suryatriyastuti *et al.* [9] studied the

56 behavior of free- and restraint-head piles in very loose sand using the pile-soil load transfer
57 approach. The proposed t - z function comprised a cyclic hardening/softening mechanism, which
58 allowed investigating the degradation of the soil/pile interface behavior under cyclic loading.
59 This approach was then compared with a numerical simulation using the finite element method
60 where the degradation of the soil-pile interface behavior under cyclic loading was considered. A
61 simulation accounting for 12 thermal cycles shows: (i) a ratcheting of pile head settlement under
62 constant working load; (ii) and a decrease in pile head load for the restraint-head pile.

63

64 Saggi & Chakraborty [12] investigated the behavior of a floating and end-bearing pile in loose
65 and dense sands under various thermal cycles by using the finite element method and nonlinear
66 transient analyses. The thermal load applied to the pile was in the same temperature range as in
67 the experiments of Laloui *et al.* [2], with a temperature amplitude of 21°C. The results show an
68 important settlement of the pile after the first thermal cycle. The subsequent thermal cycles
69 induce pile heave. This phenomenon can be clearly seen in the case of dense sand where the pile
70 and the soil surface move upward together after 50 cycles. Actually, the pile and soil were
71 progressively heated during these 50 cycles. In addition, the pile shaft resistance in dense sand
72 increases with the thermal cycles while this value does not change in loose sand. The authors
73 explain this observation in the case of dense sand by the larger horizontal stress induced by soil
74 thermal expansion which affects the mobilized pile shaft resistance. However, a parametric study
75 shows a decreasing trend of the pile axial stress with thermal cycles. A similar result can be
76 found in the numerical study of Olgun *et al.* [36] where pile head displacement and axial stress
77 were investigated under three different climatic conditions for 30 years. After 30 annual thermal
78 cycles, even if the pile was progressively cooled, its axial stress tends to increase. A decrease in

79 axial stress is observed during a heating process. This was explained by the difference in the
80 thermal dilations of the pile and the soil, respectively. Ng *et al.* [39] studied the horizontal stress
81 change of soil element close to the pile when the pile was subjected to 50 heating-cooling cycles.
82 The results show that the horizontal stress along the pile decreases with thermal cycles, this
83 decrease being particularly affected by the thermal cycles amplitude and the pile diameter.
84 Pasten & Santamarina [17] also used a modified one-dimensional load transfer model to predict
85 the long-term response of shaft- and end-bearing piles subjected to thermal cycles. They show
86 that the most plastic settlement of the pile took place during the first few cycles. More recently,
87 Vieira & Maranhã [35] investigated the behavior of a floating pile model in clay soil under
88 different load levels and seasonal temperature during five years using the finite element method.
89 The results indicate that when the pile works with a high factor of safety its displacement is
90 reversible during the thermal cycles. However, a low factor of safety induces an increase in axial
91 stresses while the rate of irreversible settlement reduces with the number of cycles.

92
93 Beside the numerical studies mentioned above, few experimental studies have been performed to
94 investigate the long-term behavior of energy piles. Ng *et al.* [24] used centrifuge modeling to
95 study the thermo-mechanical behavior of energy piles constructed in lightly and heavily over-
96 consolidated clays under five thermal cycles. The results show that the most irreversible
97 settlement of the pile is observed in the first thermal cycle. In the following cycles, the settlement
98 increases at a lower rate. After 5 cycles, the accumulated settlement is about 3.8%D (pile
99 diameter) for a pile in the lightly over-consolidated clay, and 2.1%D for heavily over-
100 consolidated clay. Another study using centrifuge modeling to investigate the long-term behavior
101 of energy pile under four thermal cycles can be found in [14]. An end-bearing pile, installed in

102 unsaturated silt, worked under a constant head load and four thermal cycles (the temperature
103 ranging from 29°C to 39°C). The observed thermal axial stress-strain behavior of the pile is in
104 agreement with the results of in-situ experiments performed by Laloui *et al.* [2], Bourne Webb *et*
105 *al.* [4] and McCartney & Murphy [40]. The profiles of axial stress, displacement and strain of
106 pile does not change significantly along the four thermal cycles.

107

108 The objective of the present study is to investigate the long-term response of a small-scale
109 energy pile. The pile model (20 mm external diameter) was installed in dry sand. 30 thermal
110 cycles were applied while the pile head load was maintained at 0, 20, 40 and 60% of the pile
111 ultimate bearing capacity. The results in terms of pile head settlement and axial force profile,
112 obtained during these thermo-mechanical loadings, are presented and discussed. Note that while
113 the long-term behavior of energy pile is usually considered under a high number of thermal
114 cycles (up to 50 cycles in the case of Ng *et al.* [39]) in numerical studies, it is usually limited to
115 few thermal cycles (up to 5 cycles in the case of Ng *et al.* [24]) in the experimental studies.

116

117 **2. Experimental method**

118 *2.1 Experimental setup*

119 A pile model (20-mm external diameter and 600-mm length) was installed in a dry sand sample
120 (548-mm inner diameter and 900-mm height) as shown in Fig. 1. The pile model is an aluminum
121 tube with an internal diameter of 18 mm and sealed at the bottom. The model pile surface was
122 coated with sand to mimic the roughness of a full-scale pile surface. The sand used in this study
123 (Fontainebleau sand) has the following physical properties: particle density $\rho_s = 2.67 \text{ Mg/m}^3$;

124 maximal void ratio $e_{max} = 0.94$; minimal void ratio $e_{min} = 0.54$; and median grain size $D_{50} = 0.23$
125 mm.

126

127 The installation process began with the compaction of two 100 mm-thick layers, then two layers
128 of 50 mm in thickness. The model pile was then installed at its position inside the soil container
129 and fixed by a steel bar fixed to the top surface of the soil container. Finally, other sand layers of
130 100 mm were compacted around the pile. The soil was compacted manually, by using a wooden
131 tamper, at a dry unit weight of 15.1 kN/m^3 .

132

133 During the compaction, three temperature sensors and two pressure gauges were installed as
134 showed in Fig. 1. The two pressure gauges (P1 & P2) locate at 50 mm below the pile toe. P1
135 measures the horizontal pressure and P2 measures the vertical pressure of soil. The three soil
136 temperature sensors (S5-S7) are placed at 300 mm below the soil surface and at three distances
137 from the pile axis, 20, 40 and 80 mm, respectively. In order to measure the pile axial strain, five
138 strain gauges (G1-G5) are distributed along the pile length. Three displacement transducers
139 (LVDT) are used to measure the pile head displacement, and a load cell records the pile head
140 load. The pile head load is controlled by the water level in a tank placed above the pile. A
141 metallic U-tube, connected to a temperature-controlled bath, is placed inside the pile tube for
142 heating and cooling the pile. The thermal conductivity of this latter is improved by filling the pile
143 tube with water. A temperature sensor (S1) is placed inside the pile to measure its temperature.
144 The soil container is thermally isolated to avoid heat exchange with the ambient air.

145

146 *2.2 Test program*

147 In this study, three tests have been performed. After each experiment, the pile model was
148 reinstalled according to the procedure described above. The first two tests T1 and T2 were
149 performed to investigate the behavior of the pile under mechanical loading and isothermal
150 conditions. The test procedure follows the French Standard [41]. In the preparation step, the pile
151 was first loaded to 50 N (10% of the pile resistance, which is 500 N, after Yavari *et al.* [21]) and
152 then unloaded to remove the disturbed settlement component due to soil compaction related to
153 the pile installation process. After this step, the pile was loaded in steps of 50 N up to 250 N
154 (50% of the pile resistance), and then unloaded completely. Finally, the pile was loaded in steps
155 of 50 N up to failure (corresponding, by convention, to a pile head settlement equal to 2 mm, *i.e.*
156 10% of the pile diameter). Each loading step was maintained for 60 min.

157

158 For the test T3, after the preparation step, the pile temperature was fixed at 20°C (similar to the
159 room temperature) for two days to ensure the homogeneity of the soil and pile temperature at the
160 initial state. After this phase, the pile was first heated from 20°C to 21°C for 4 h and then cooled
161 to 19°C for 4 h. Finally, the initial temperature of 20°C was imposed to the pile for at least 16 h.
162 Thus the total duration of one thermal cycle equals to 24 h. 30 thermal cycles were applied
163 during this first stage. In the subsequent stage, an axial head load of 100 N (20% of the pile
164 resistance) was applied. 30 thermal cycles were then applied under this pile head load. The same
165 procedure was repeated at pile head loads of 200 N and 300 N (40% and 60%, respectively, of
166 the pile resistance). The thermo-mechanical loading path of the test T3 is summarized in Fig. 2.

167

168 **3. Results**

169 Fig 3 shows the results obtained for the test T1. The pile head settlement is plotted against
170 elapsed time for each loading step. The pile head settles immediately after the application of the
171 axial load. Afterwards, the settlement increases with time but at a lower rate. In general, the
172 relationship between the pile head settlement and the logarithm of time can be fitted using a
173 linear function (for the last 30 min of each loading step). That function allows determining the
174 creep rate as shown in equation (1).

$$175 \quad \alpha = (S_{60} - S_{30})/\log(60/30) \quad (1)$$

176 where α is the creep rate; S_{60} and S_{30} are the settlements of the pile head at 60 min and 30 min,
177 respectively. Fig. 4 shows the creep rate of all the three tests. It can be observed that the higher
178 the pile head load the higher the creep rate, and that a linear function fits satisfactorily the
179 relationship between these two quantities. The results of the three tests are quite similar showing
180 the good repeatability of the experimental procedure. Other results concerning the mechanical
181 behavior of the pile under mechanical loading are similar to that obtained by Yavari *et al.* [21] by
182 using the same experimental setup and by testing the same sand. For this reason, these results
183 (pile head settlement versus pile head load, pile axial stress profile, *etc.*) are not shown in the
184 present paper. Only the results on creep rate are shown here because such results were not shown
185 in the work of Yavari *et al.* [21] and they are important when investigating the long-term
186 behavior of piles.

187

188 Fig. 5 shows the temperature measured at various locations together with the pile head settlement
189 after the first heating-cooling cycle in the test T3 under a constant head load corresponding to
190 20% of the pile resistance. When the temperature of the pile is increased from 20°C to 21°C, the
191 soil temperature at 20 mm (S5), 40 mm (S6), and 80 mm (S7) from the center of the pile

192 increases subsequently. But the temperature change at 80 mm remains very small. It seems that
193 the duration of 4 h for the heating phase is long enough for the soil temperature to reach
194 equilibrium. The same conclusion can be drawn for the subsequent cooling phase (pile
195 temperature is decreased to 19°C) and the final heating phase (pile temperature is increased to its
196 initial value, 20°C). The results on the pile head settlement show that heating does not induce
197 any significant movement but that cooling induces a settlement (the normalized settlement is the
198 ratio between the pile head settlement and the pile diameter). In addition, the pile head settlement
199 and the pile temperature stabilize at the same time.

200

201 In Fig. 6, the pile head settlement is plotted versus the pile temperature change during the first
202 heating-cooling cycle for the four axial loads. It can be observed that the pile behavior depends
203 on the mechanical load applied to it. The pile head heave associated to heating can only be
204 observed when the pile is free of load (Fig. 6a). In this case, the displacement of the pile head is
205 similar to the pile's thermal expansion curve, which corresponds to the temperature-induced
206 deformation of a pile restrained at its toe but free to move at its head. In the three other cases, the
207 pile head does not move during the initial heating phase. The subsequent cooling phase induces a
208 settlement in all the four cases. The slope of the settlement is similar to the thermal expansion
209 curve. The final heating phase, when temperature increases back to the initial temperature, does
210 not induce any displacement in all the four cases. As a result, the first heating/cooling cycle
211 induces irreversible pile head settlement in all the four cases. In addition, the higher is the axial
212 load, the higher the irreversible settlement. This phenomenon is similar to that observed by
213 Kalantidou *et al.* [7] and Yavari *et al.* [21] on dry sand and Yavari *et al.* [18] on saturated clay.

214

215 In Fig. 7, the irreversible pile head settlement and its ratio to the pile diameter (normalized
216 settlement) are plotted versus the number of thermal cycles for all the four axial pile head loads.
217 When pile is free of load, the irreversible settlement is negligible. In the other cases, the higher is
218 the pile head load, the more important is the observed settlement. In addition, for a given pile
219 head load, the irreversible settlement increases with the number of thermal cycles, while tending
220 to stabilize for a high number of cycles. In addition, while the irreversible pile head settlement
221 tends to stabilize after around 20 cycles for low pile head load (up to 40% of pile resistance),
222 under higher pile head loads (60% of pile resistance), it continues to increase at a constant rate
223 over the 30 applied thermal cycles.

224

225 For a deeper analysis of the pile head settlement with thermal cycles the irreversible pile head
226 settlement was calculated using the following equation (see Pasten & Santamarina [17]):

$$227 \delta_1 = \delta_1|_{N_c \rightarrow \infty} (1 - \exp(-\beta \cdot N_c)) \quad (2)$$

228 Here, δ_l is the irreversible pile head displacement; N_c is the number of cycles; β is a model
229 parameter obtained by fitting the experimental data (one value per pile head load). The result in
230 Fig. 7 shows that this equation can fit correctly all the experimental data.

231

232 Besides, irreversible settlement was also normalized with respect to the settlement obtained
233 during the first cycle as suggested by Suryatriyastuti *et al.* [9]. This ratio of pile settlement is
234 plotted versus the number of cycles in Fig. 8 for all the four pile head loads. The results show
235 that this ratio increases quickly during the first ten cycles and then tends to stabilize at a high
236 number of cycle. Note that in the study of Suryatriyastuti *et al.* [9], at a pile head load of 33% of

237 the pile resistance, 12 heating/cooling cycles induce a ratio of approximately 1.2. This value is
238 similar to the one found in the present work for the case of 40% of the pile resistance.

239
240 The results on the axial force along the pile, measured by the strain gages and the pile head load
241 sensor, are plotted in Fig. 9. The axial force Q is normalized with respect to the pile resistance
242 $Q_{ult} = 500$ N and the depth z is normalized with respect to the pile length $H = 600$ mm. At the
243 initial state, when no pile head load is applied, the axial force along the pile remains smaller than
244 5% of Q_{ult} . The subsequent thermal cycles do not significantly modify the axial force. When a
245 load of 20% of Q_{ult} is applied to the pile head, the axial force along the pile also increases.
246 Afterwards, the first heating phase leads to a slight increase of the axial force and the subsequent
247 cooling phase leads to a slight decrease. After 30 cycles of heating/cooling, the axial force is
248 higher than the initial one (under mechanical load). Note that the axial force after the 30th heating
249 phase is also higher than that after the 30th cooling phase. The cases of loads corresponding to
250 40% and 60% of Q_{ult} lead to similar observations.

251
252 Fig. 10 shows the pile head load, the horizontal and vertical pressures in soil at 50 mm under the
253 pile toe as a function of the number of thermal cycles. The initial stress (10 kPa and 5 kPa for
254 vertical and horizontal ones, respectively) corresponds to the weight of the soil specimen. The
255 coefficient of horizontal pressure at rest of 0.5 is in the usual range for dry sand [12, 21, 42].
256 These pressures increased significantly when the pile head load was increased but the thermal
257 cycles did not influence these values.

258

259 In Fig. 11, the irreversible settlement of the pile head measured after 30 thermal cycles is plotted
260 versus the pile head load. In this figure, the pile head settlement, estimated from the creep rate
261 (shown in Fig. 4) and the duration of the thermal phase, is also plotted. The difference between
262 these two values can be attributed to the settlement related uniquely to the thermal cycles. It can
263 be seen that the settlement related to thermal cycles is much larger than that related to creep. The
264 higher is the pile head load, the higher is the irreversible settlement.

265

266 **4. Discussion**

267 In the present work, the temperature variation was imposed at $\pm 1^\circ\text{C}$. This range is much smaller
268 than the temperature variation of the energy piles which can reach up to $\pm 20^\circ\text{C}$ [2, 4, 11, 21, 25,
269 27]. Actually, in this small-scale model, the dimension of the pile is 20 times smaller than a full-
270 scale pile of 0.4 m in diameter and 12 m length. As a consequence, the strain related to the
271 mechanical load is 20 times smaller than that at the full scale [2, 8, 11, 24]. For this reason, the
272 temperature variation was reduced 20 times in order to have a thermal dilation of the pile 20
273 times smaller than that at the full scale. The thermo-mechanical behavior of the pile observed at
274 the small scale can then be used to predict the behavior of energy piles at the full scale.

275

276 The irreversible evolution of the pile head settlement with thermal cycles observed in the present
277 work (Fig. 7) is similar to that obtained by Ng *et al.* [24] on saturated clay using centrifuge
278 modeling. These authors applied five thermal cycles and observed a ratcheting of pile head
279 settlement. A similar behavior can be found in the numerical study of Vieira & Maranhã [35]. In
280 the present work, with 30 thermal cycles (which can represent 30 years of seasonal temperature
281 changes of energy piles), the results confirm that the increment of irreversible settlement per

282 cycle is higher during the first cycles but becomes negligible after 20 cycles for the cases of axial
283 loads lower than 40% of the pile resistance (which corresponds to the service load of piles in real
284 cases). The irreversible settlement continues to increase after 20 cycles only when the pile head
285 load is high (60% of the pile resistance).

286

287 When comparing the results obtained in the present work to those obtained in the numerical
288 work of Pasten & Santamarina [17], common trends can be found, as shown in Fig. 7. The
289 parameter β represents the shape of the curve. The results obtained do not show a clear trend in
290 the relationship between this parameter and the pile head load. A similar conclusion can be
291 drawn from the Fig. 8 where the irreversible pile head settlement is normalized with respect to its
292 value after the first thermal cycle. The mechanisms considered is the work of Suryatriyastuti et
293 al. [9] can be used to explain the results obtained in the present work. These authors embedded a
294 strain hardening/softening mechanism at the pile-soil interface into the proposed t - z function to
295 consider cyclic degradation effects during the thermal cycles. The numerical investigation of Ng
296 *et al.* [39] also confirms the decrease in resistance of pile-soil interface versus the number of
297 thermal cycles. In addition, Vargas & McCarthy [43] show that thermal cycles induce thermal
298 volume change of grains, which can lead to compaction under constant stress. These authors
299 explain this structural rearrangement by the thermal effect generating an increase in the average
300 contact forces between soil particles. In addition, Fityus [44] studied the behavior of a model
301 footing on expansive clay under wetting/drying cycles and found a similar trend as far as the
302 accumulating irreversible settlement is concerned.

303

304 The study of Saggu & Chakraborty [12] shows an opposite trend compared with the present
305 experiment. Actually, the axial stress decreased after fifty cycles and the pile settlement was
306 observed only in the first thermal cycle. This phenomenon was explained by the stress transfer
307 into the surrounding soil, and the progressive heating of pile with thermal cycles.

308
309 Figure 9 shows an increase of the axial force along the pile when the number of thermal cycles
310 increases. This behavior is similar to that predicted by numerical approaches ([9, 17, 35]).
311 Actually, in these studies, this behavior can be explained by the degradation of the pile-soil
312 interface resistance with the accumulating cycles. In a different case, Pasten & Santamarina [17]
313 show the axial force profile of pile during fifty cycles. The axial force along the pile was larger
314 in the heating phase than in the cooling phase. However, the axial force in the cooling phase was
315 similar to that at the initial state.

316
317 Fig. 11 shows that the thermal settlement response of pile head shows a trend similar to the result
318 from the study of Yavari *et al.* [18] and Vieira & Maranhã [35]. Especially, all these studies have
319 investigated the thermal response of a pile when it works under different constant head loads.
320 The results showed that the long-term performance of energy piles induced significant
321 irreversible settlement and that the thermal settlement is greater at higher constant head loads.

322

323 **5. Conclusions**

324 The long-term behavior of energy piles was investigated using a small-scale model. 30
325 heating/cooling cycles were applied to the model pile under various constant pile head loads
326 varying from 0 to 60% of pile resistance. The following conclusions can be drawn:

- 327 - Thermal cycles under constant head load induces irreversible settlement of the pile head
- 328 - The irreversible settlement of the pile head is higher at a higher pile head load
- 329 - The first thermal cycle induces the highest irreversible pile head settlement. The
330 incremental irreversible settlement, accumulating after each thermal cycle, decreases
331 when the number of cycles increases. It becomes negligible at high number of thermal
332 cycles and/or low pile head load. The evolution of irreversible pile head settlement versus
333 the number of cycles can be reasonably predicted by an asymptotic equation.
- 334 - The axial force measurement along the pile increases progressively with the increase of
335 the number of thermal cycles. The axial force at the end of a heating phase is higher than
336 that at the end of the subsequent cooling phase.

337 The results obtained in the present work could be helpful to predict the long-term settlement of a
338 building having all the foundation piles equipped with a heat exchanger system. A similar test
339 program should be conducted on full-scale piles, for further researches, in order to confirm
340 quantitatively these observations. In general, the results suggest that the stress/strain behavior of
341 energy piles would continue to evolve even several years after their installation.

342

343 **References**

- 344 1. Brandl H (2006) Energy foundations and other thermo-active ground structures.
345 *Géotechnique* 56:81–122. doi: 10.1680/geot.2006.56.2.81
- 346 2. Laloui L, Nuth M, Vulliet L (2006) Experimental and numerical investigations of the
347 behaviour of a heat exchanger pile. *Int J Numer Anal Methods Geomech* 30:763–781. doi:
348 10.1002/nag.499
- 349 3. Adam D, Markiewicz R (2009) Energy from earth-coupled structures, foundations,
350 tunnels and sewers. *Géotechnique* 59:229–236.
- 351 4. Bourne-Webb PJ, Amatya B, Soga K, et al (2009) Energy pile test at Lambeth College,
352 London: geotechnical and thermodynamic aspects of pile response to heat cycles.
353 *Géotechnique* 59:237–248. doi: 10.1680/geot.2009.59.3.237

- 354 5. McCartney JS, Rosenberg JE (2011) Impact of Heat Exchange on Side Shear in Thermo-
355 Active Foundations. *Geo-Frontiers 2011* © ASCE 2011 488–498.
- 356 6. Amatya BL, Soga K, Bourne-Webb PJ, et al (2012) Thermo-mechanical behaviour of
357 energy piles. *Géotechnique* 62:503–519. doi: 10.1680/geot.10.P.116
- 358 7. Kalantidou A, Tang AM, Pereira J-M, Hassen G (2012) Preliminary study on the
359 mechanical behaviour of heat exchanger pile in physical model. *Géotechnique* 62:1047–
360 1051. doi: 10.1680/geot.11.T.013
- 361 8. Murphy KD, Mccartney JS, Henry KS, Fellow LF (2014) Thermo-Mechanical
362 Characterization of a Full-Scale Energy Foundation. In: *From Soil Behav. Fundam. to*
363 *Innov. Geotech. Eng. Atlanta, Georgia, United states*, pp 617–628
- 364 9. Suryatriyastuti ME, Mroueh H, Burlon S (2014) A load transfer approach for studying the
365 cyclic behavior of thermo-active piles. *Comput Geotech* 55:378–391. doi:
366 10.1016/j.compgeo.2013.09.021
- 367 10. Di Donna A, Laloui L (2015) Numerical analysis of the geotechnical behaviour of energy
368 piles. *Int J Numer Anal Methods Geomech* 39:861–888. doi: 10.1002/nag.2341
- 369 11. Wang B, Bouazza A, Singh RM, et al (2014) Posttemperature Effects on Shaft Capacity of
370 a Full-Scale Geothermal Energy Pile. *J Geotechnol Geoenvironmental Eng* 141:04014125.
371 doi: 10.1061/(ASCE)GT.1943-5606.0001266.
- 372 12. Saggi R, Chakraborty T (2015) Cyclic Thermo-Mechanical Analysis of Energy Piles in
373 Sand. *Geotech Geol Eng* 33:321–342. doi: 10.1007/s10706-014-9798-8
- 374 13. Akrouch GA, Sánchez M, Briaud J-L (2014) Thermo-mechanical behavior of energy piles
375 in high plasticity clays. *Acta Geotech* 9:399–412. doi: 10.1007/s11440-014-0312-5
- 376 14. Stewart MA, McCartney JS (2013) Centrifuge Modeling of Soil-Structure Interaction in
377 Energy Foundations. *J Geotech Geoenvironmental Eng* 140:04013044. doi:
378 10.1061/(ASCE)GT.1943-5606.0001061
- 379 15. Mimouni T, Laloui L (2015) Behaviour of a group of energy piles. *Can Geotech J*
380 52:1913–1929. doi: 10.1139/cgj-2014-0403
- 381 16. Salciarini D, Ronchi F, Cattoni E, Tamagnini C (2015) Thermomechanical Effects
382 Induced by Energy Piles Operation in a Small Piled Raft. 15:1–14. doi:
383 10.1061/(ASCE)GM.1943-5622.0000375.
- 384 17. Pasten C, Santamarina JC (2014) Thermally Induced Long-Term Displacement of
385 Thermoactive Piles. *J Geotech Geoenvironmental Eng* 140:06014003. doi:
386 10.1061/(ASCE)GT.1943-5606.0001092
- 387 18. Yavari N, Tang AM, Pereira J, Hassen G (2016) Mechanical behaviour of a small-scale
388 energy pile in saturated clay. *Géotechnique*. doi: 10.1680/geot/15-7-026
- 389 19. Yavari N, Tang AM, Pereira JM, Hassen G (2016) Effect of temperature on the shear

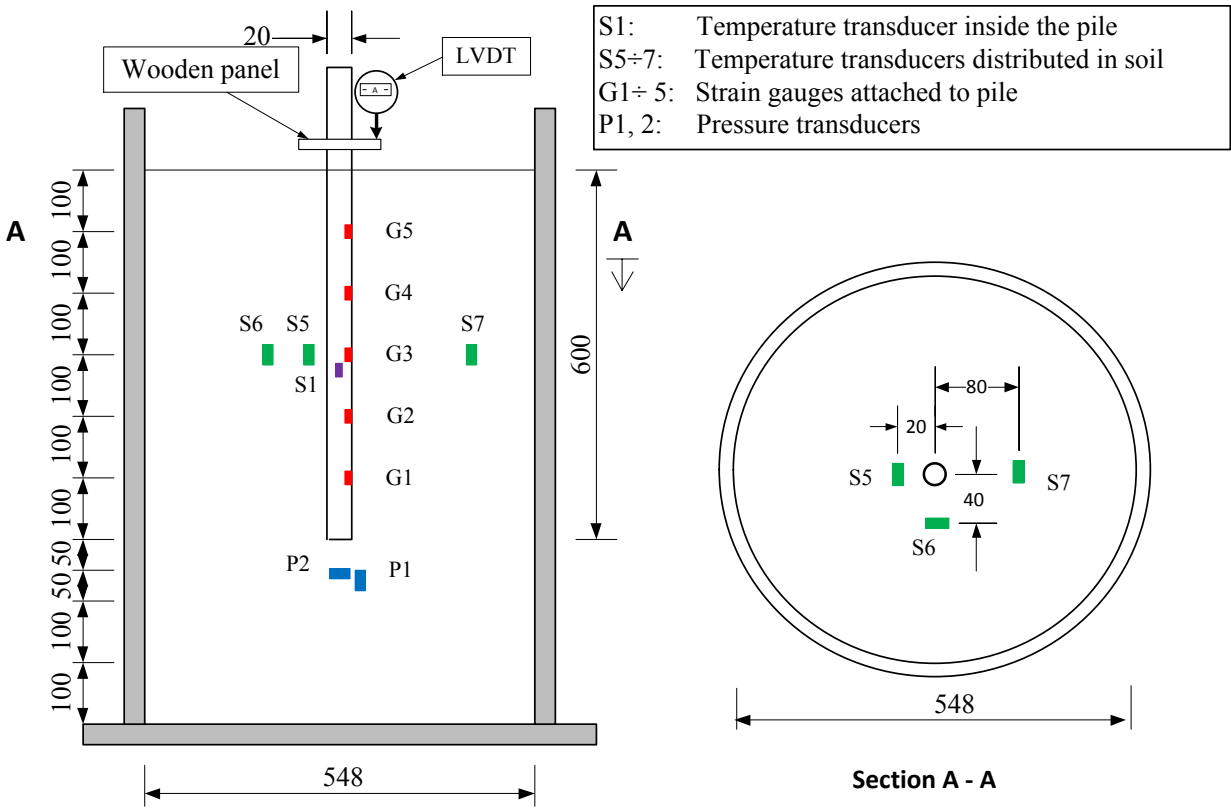
- 390 strength of soils and soil/structure interface. *Can Geotech J* 59:1–9. doi: 10.1139/cgj-
391 2015-0355
- 392 20. Yavari N, et al (2013) A simple method for numerical modelling of mechanical behaviour
393 of an energy pile. *Géotechnique Lett*. doi: 10.1680/geolett. 13.00053
- 394 21. Yavari N, Tang AM, Pereira J-M, Hassen G (2014) Experimental study on the mechanical
395 behaviour of a heat exchanger pile using physical modelling. *Acta Geotech* 9:385–398.
396 doi: 10.1007/s11440-014-0310-7
- 397 22. Stewart MA, Asce SM, McCartney JS, et al (2014) Centrifuge Modeling of Soil-Structure
398 Interaction in Energy Foundations. *J Geotech Geoenvironmental Eng* 140: 04013044 . doi:
399 10.1061/(ASCE)GT.1943-5606.0001061.
- 400 23. Lam SY, Ng CWW, Leung CF, Chan SH (2009) Centrifuge and numerical modeling of
401 axial load effects on piles in consolidating ground. *Can Geotech J* 46:10–24. doi:
402 10.1139/T08-095
- 403 24. Ng CWW, Shi C, Gunawan A, Laloui L (2014) Centrifuge modelling of energy piles
404 subjected to heating and cooling cycles in clay. *Géotechnique Lett* 4:310–316. doi:
405 10.1680/geolett.14.00063
- 406 25. Ng CWW, Shi C, Gunawan A, et al (2014) Centrifuge modelling of heating effects on
407 energy pile performance in saturated sand. *Can Geotech J* 52:1045–1057. doi:
408 10.1139/cgj-2014-0301
- 409 26. Murphy KD, McCartney JS, Henry KS (2014) Evaluation of thermo-mechanical and
410 thermal behavior of full-scale energy foundations. *Acta Geotech* 10:179–195. doi:
411 10.1007/s11440-013-0298-4
- 412 27. Murphy KD, McCartney JS (2014) Seasonal Response of Energy Foundations During
413 Building Operation. *Geotech Geol Eng* 33(2):343–356. doi: 10.1007/s10706-014-9802-3
- 414 28. Laloui L, Nuth M (2006) Numerical Modeling of some features of heat exchanger pile.
415 *Geotech Spec Publ* 153:189. doi: 10.1061/40865(197)24
- 416 29. Jeong S, Lim H, Lee JK, Kim J (2014) Thermally induced mechanical response of energy
417 piles in axially loaded pile groups. *Appl Therm Eng* 71:608–615. doi:
418 10.1016/j.applthermaleng.2014.07.007
- 419 30. Di Donna A, Rotta Loria AF, Laloui L (2016) Numerical study of the response of a group
420 of energy piles under different combinations of thermo-mechanical loads. *Comput*
421 *Geotech* 72:126–142. doi: 10.1016/j.compgeo.2015.11.010
- 422 31. Murphy KD, McCartney JS, Henry KS (2014) Evaluation of thermo-mechanical and
423 thermal behavior of full-scale energy foundations. *Acta Geotech*. 10:179-195. doi:
424 10.1007/s11440-013-0298-4
- 425 32. Akrouch GA, Sánchez M, Briaud J-L (2014) Thermo-mechanical behavior of energy piles
426 in high plasticity clays. *Acta Geotech* 9(3):399–412. doi: 10.1007/s11440-014-0312-5

- 427 33. Mimouni T, Laloui L (2014) Towards a secure basis for the design of geothermal piles.
428 Acta Geotech 9:355–366. doi: 10.1007/s11440-013-0245-4
- 429 34. Loria AFR, Donna A Di, Ph D, Laloui L (2015) Numerical Study on the Suitability of
430 Centrifuge Testing for Capturing the Thermal-Induced Mechanical Behavior of Energy
431 Piles. J Geotech Geoenvironmental Eng 141:04015042. doi: 10.1061/(ASCE)GT
- 432 35. Vieira A, Maranhã JR (2016) Thermoplastic Analysis of a Thermoactive Pile in a
433 Normally Consolidated Clay. Int J Geomech 1–21. doi: 10.1061/(ASCE)GM.1943-
434 5622.0000666.
- 435 36. Olgun CG, Ozudogru TY, Abdelaziz SL, Senol A (2015) Long-term performance of heat
436 exchanger piles. Acta Geotech 10:553–569. doi: 10.1007/s11440-014-0334-z
- 437 37. Wang W, Regueiro RA, McCartney JS (2015) Coupled axisymmetric thermo-poro-
438 elasto-plastic finite element analysis of energy foundation centrifuge experiments in
439 partially saturated silt. Geotech Geol Eng 33:373–388. doi: 10.1007/s10706-014-9801-4
- 440 38. Dupray F, Laloui L, Kazangba A (2014) Computers and Geotechnics Numerical analysis
441 of seasonal heat storage in an energy pile foundation. Comput Geotech 55:67–77. doi:
442 10.1016/j.compgeo.2013.08.004
- 443 39. Ng CWW, Ma QJ, Gunawan A (2016) Horizontal stress change of energy piles subjected
444 to thermal cycles in sand. Comput Geotech 78:54–61. doi:
445 10.1016/j.compgeo.2016.05.003
- 446 40. McCartney JS, Murphy KD (2012) Strain Distributions in Full-Scale Energy Foundations (
447 DFI Young Professor Paper Competition 2012). DFI J J Deep Found Inst 6:26–38.
- 448 41. NF P 94-150-1 (1999) Essai statique de pieu isolé sous un effort axial. 1–28.
- 449 42. Mayne PW, Kulhawy FH (1982) K_0 - OCR Relationships in Soil. J Geotech Eng Div
450 108:851–872.
- 451 43. Vargas WL, McCarthy JJ (2007) Thermal expansion effects and heat conduction in
452 granular materials. Phys Rev E - Stat Nonlinear, Soft Matter Phys 76:1–8. doi:
453 10.1103/PhysRevE.76.041301
- 454 44. Fityus S (2003) Behaviour of a model footing on expansive clay. In: Proc. Unsat Asia
455 2003, 2nd Asian Unsaturated Soils Conf. Osaka, pp 181–186

456

457

458

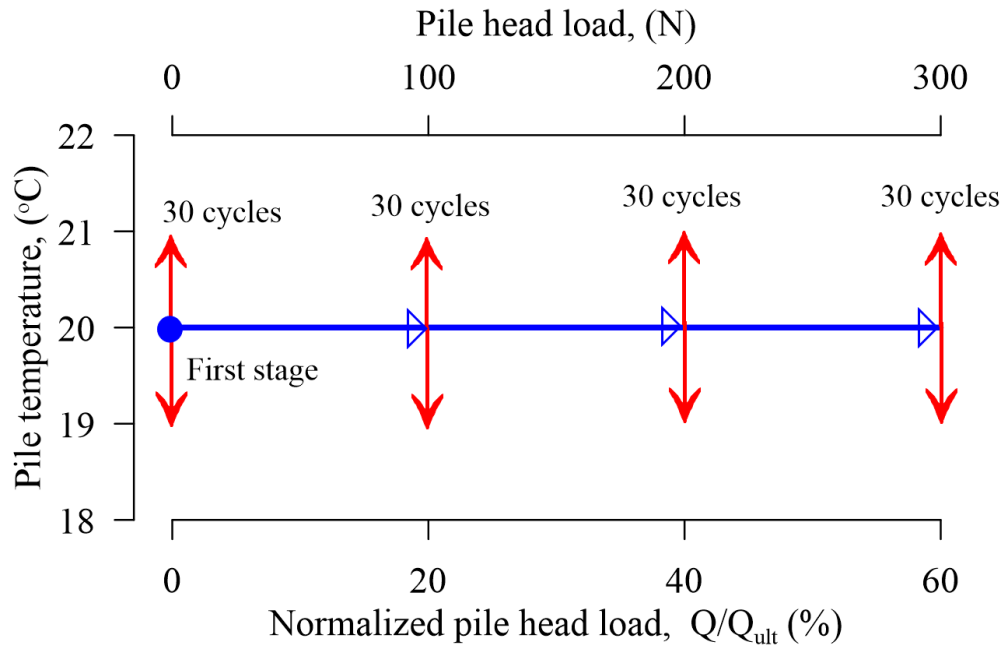


460

461 Fig. 1 Experiment setup

462

463

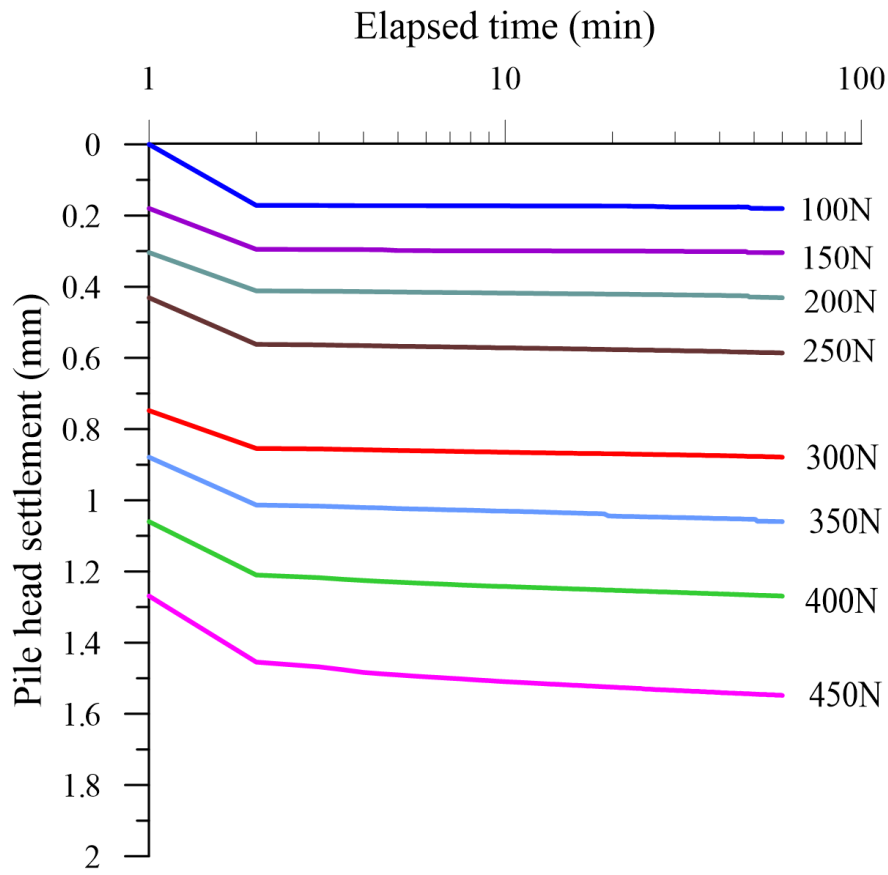


464

465 Fig. 2 Thermo-mechanical loading path of the test T3.

466

467

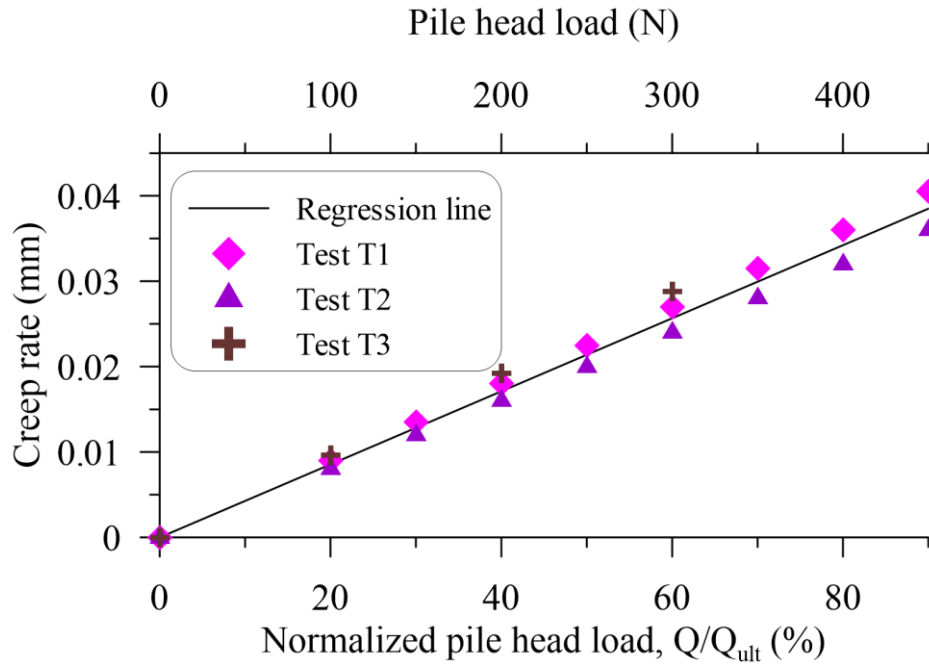


468

469 Fig. 3 Mechanical settlement of pile in test T1

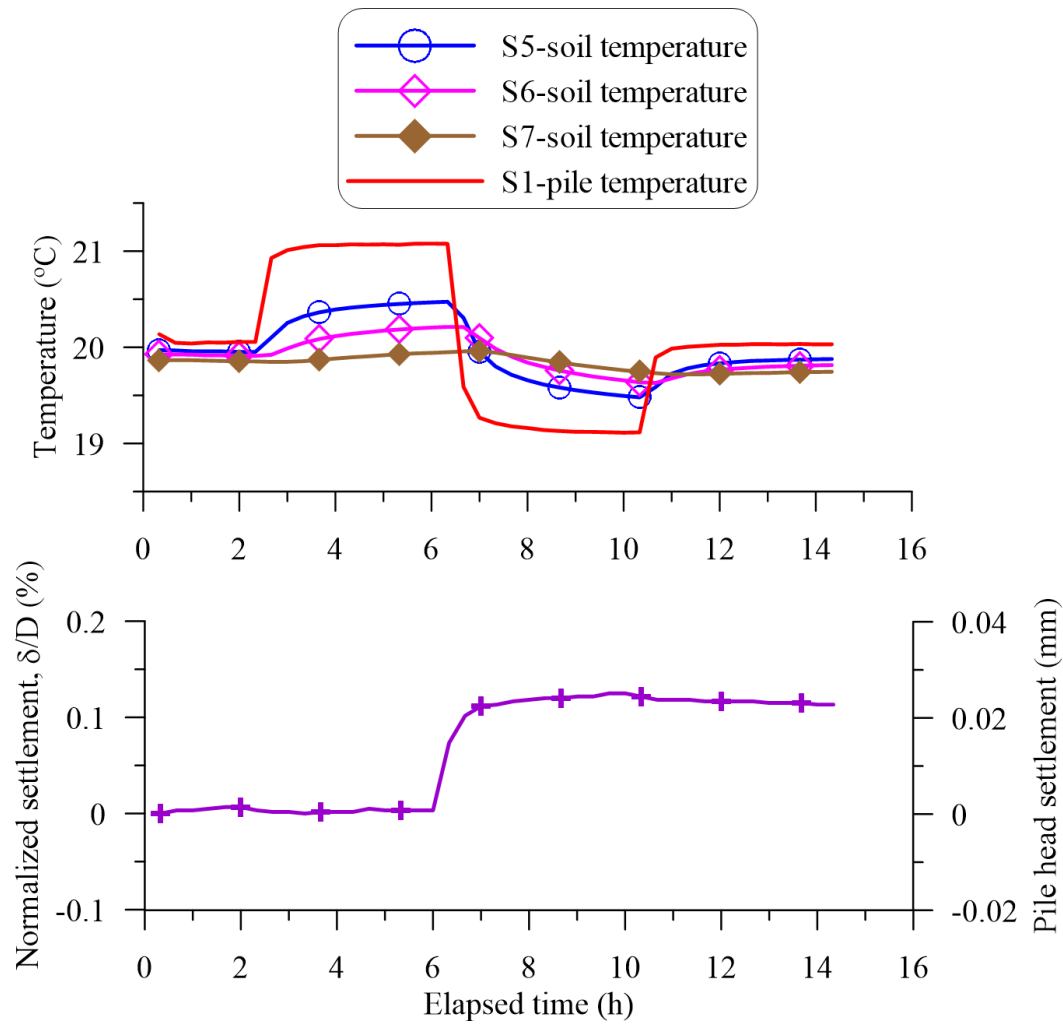
470

471



472

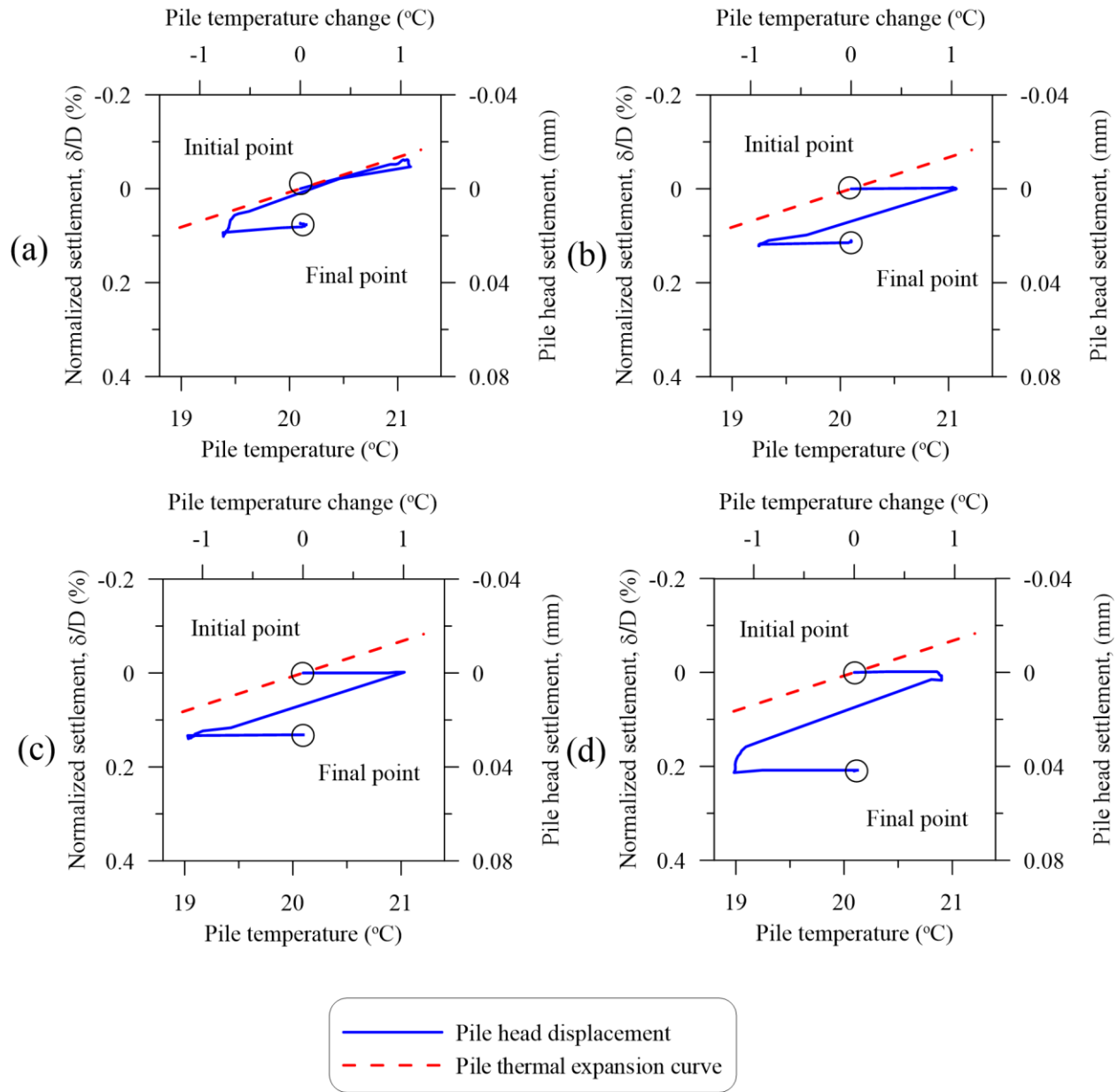
473 Fig. 4 Creep behavior of pile for all the three tests.



474

475 Fig. 5 Pile head settlement, soil and pile temperature versus elapsed time during the first thermal

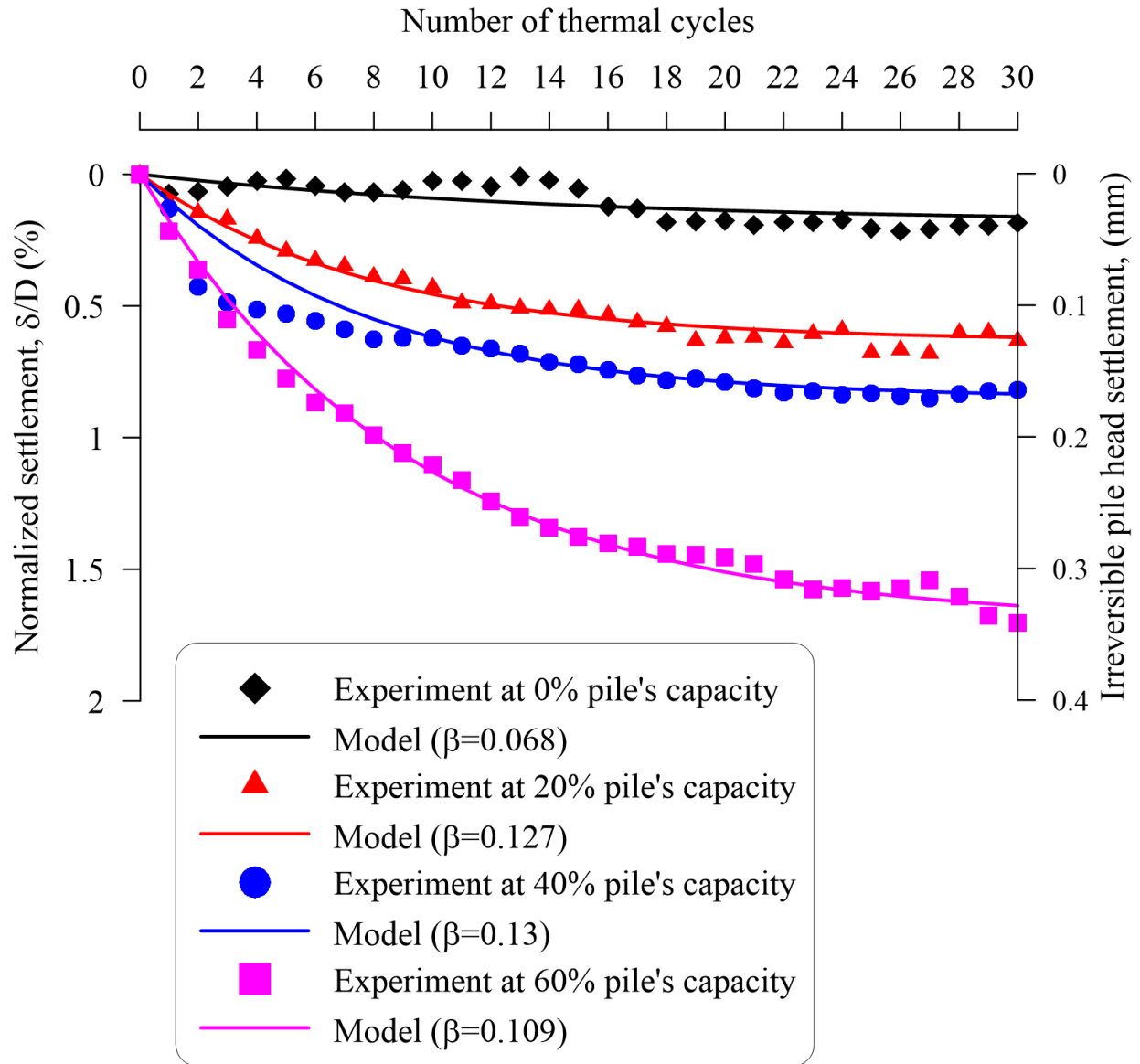
476 cycle at 20% of pile resistance.



477

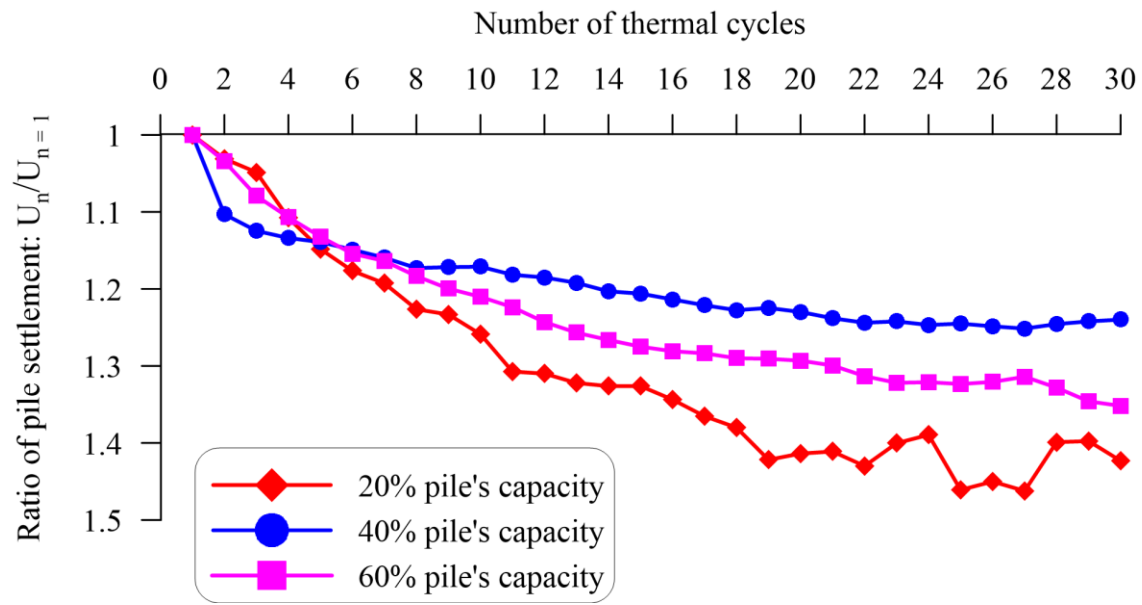
478 Fig. 6 Pile head settlement versus temperature change during the first cycle at axial load of (a)

479 0%; (b) 20%; (c) 40%; (d) 60% of pile resistance.



480

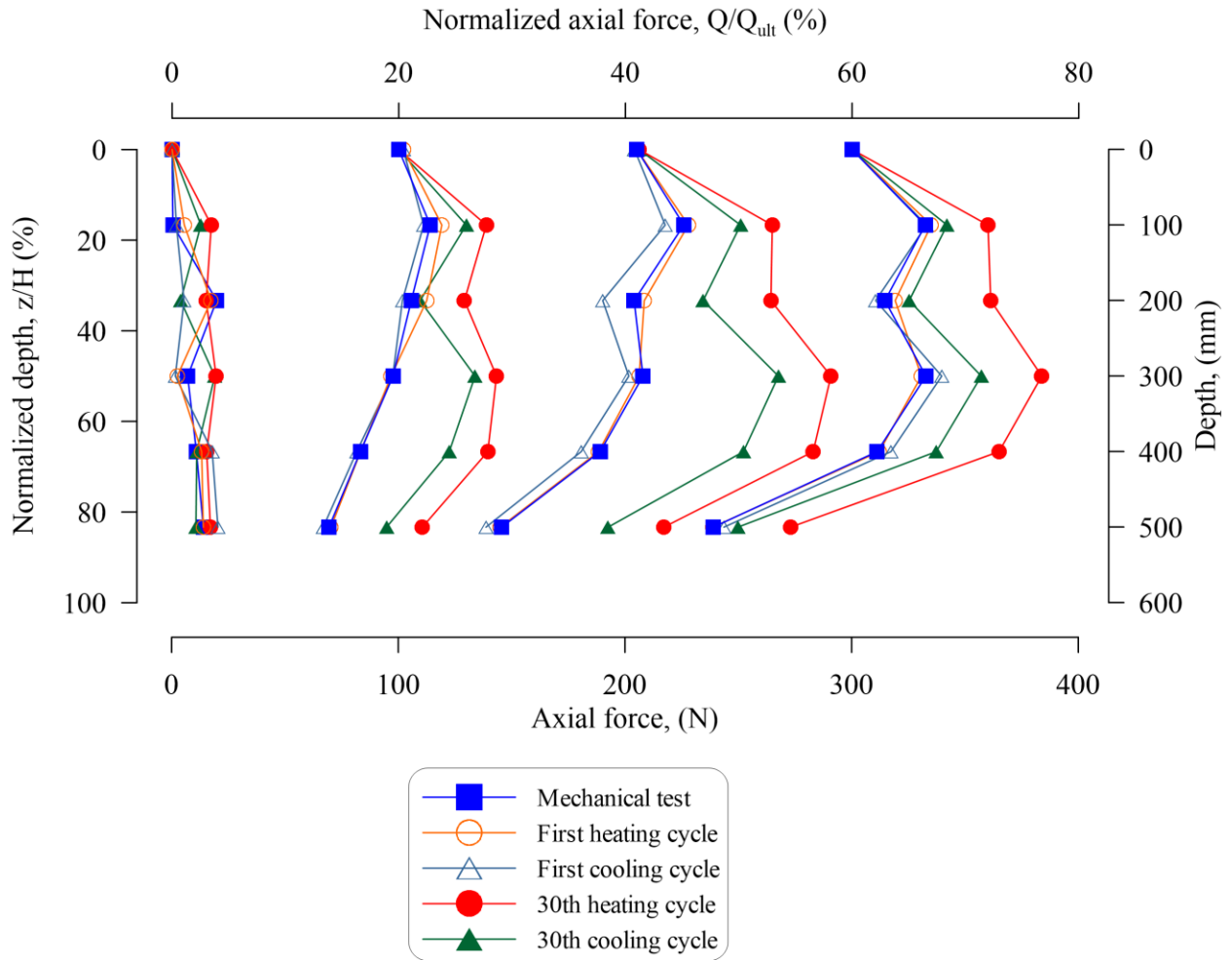
481 Fig. 7 Irreversible pile head settlement versus number of thermal cycles.



482

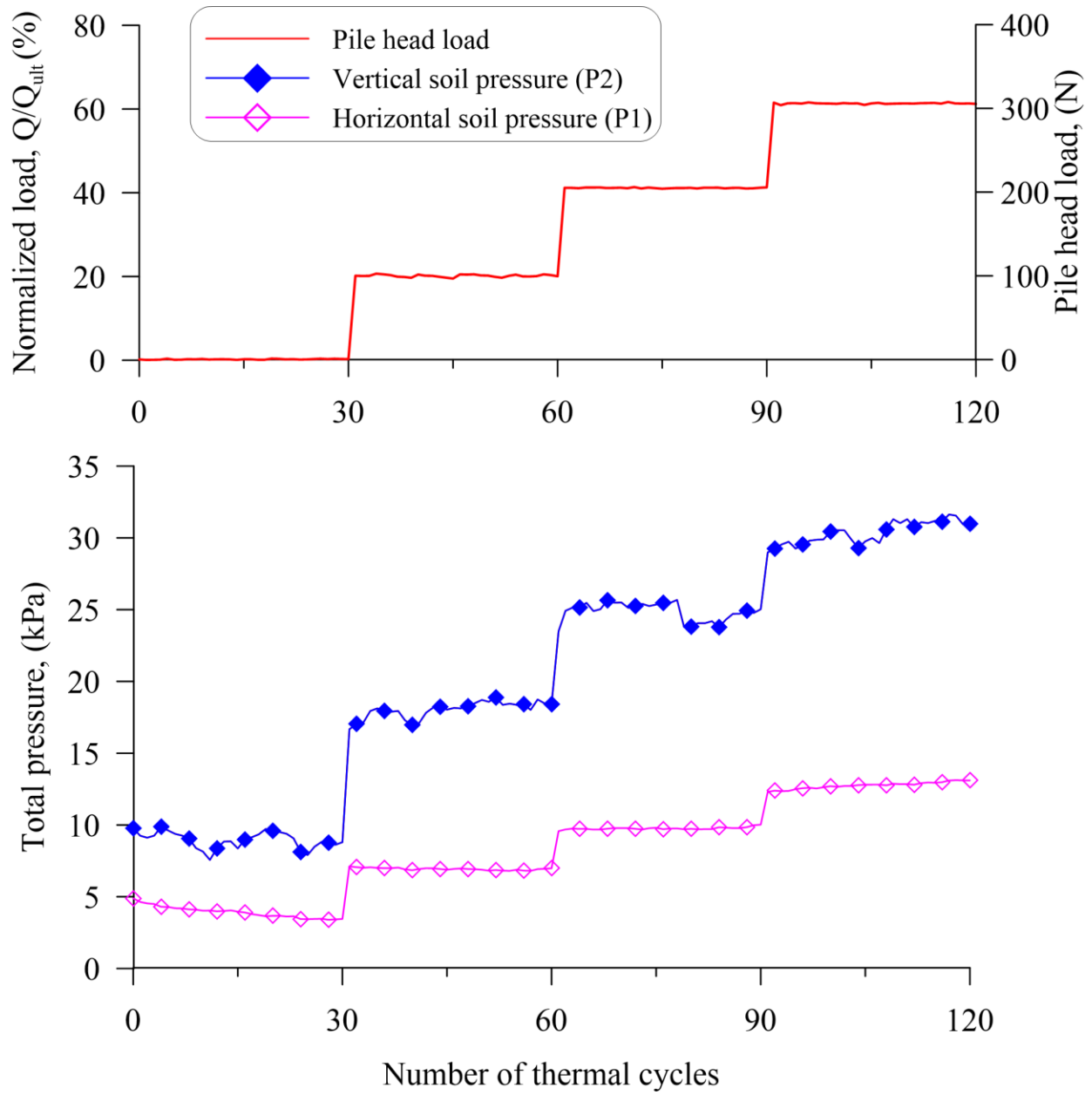
483 Fig. 8 Ratio of pile settlement versus number of cycles.

484



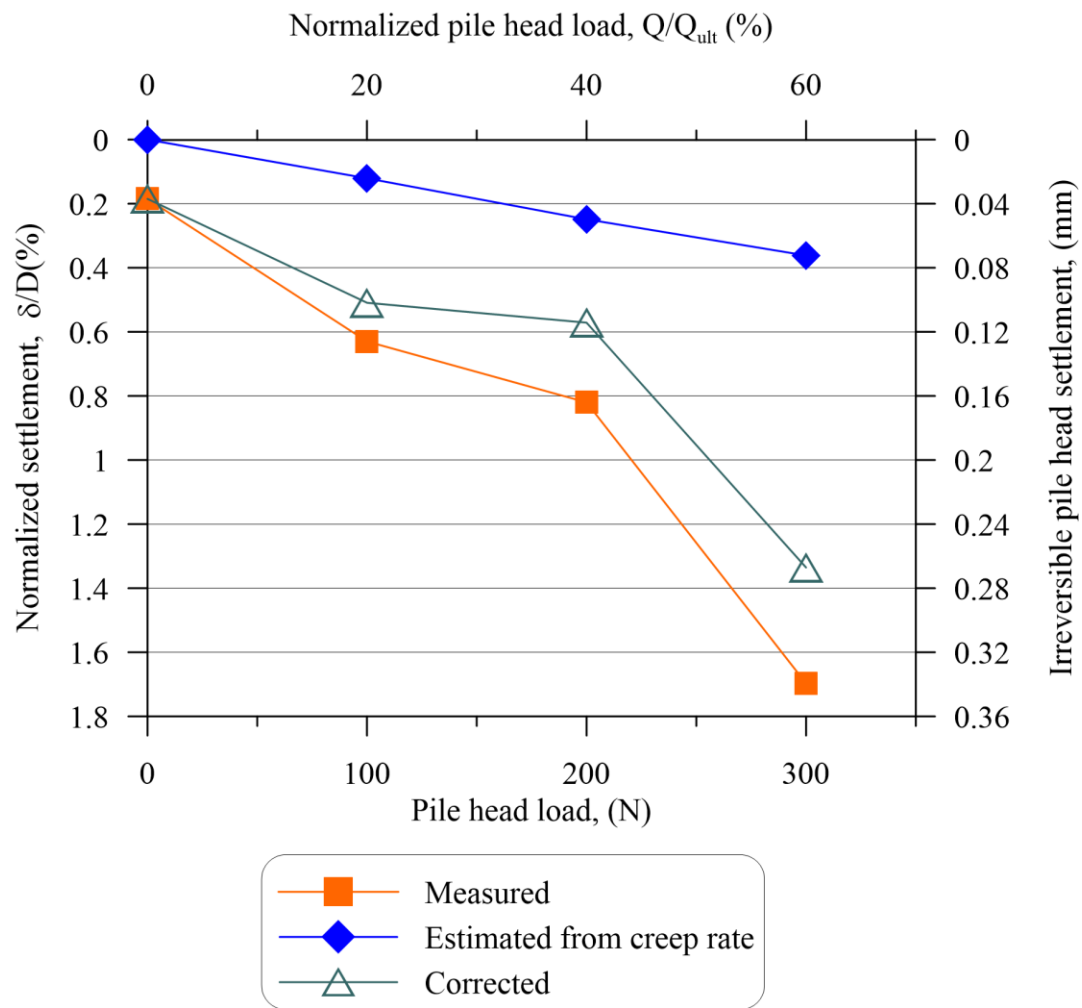
485

486 Fig. 9 Axial force profile during thermal cycles



487

488 Fig. 10 Pile head load and total pressures in soil versus number of thermal cycles



489

490 Fig. 11 Pile head settlement after 30 cycles versus pile head load